Estimating Automobile Chassis Voltage Distortion Using Load Currents

Christopher R. Laughman   Steven R. Shaw   Steven B. Leeb

***Abstract*— This paper provides a model of the automobile chassis impedance for the purposes of predicting voltage distortion. A discrete-time model of the chassis and a method for identifying its parameters is introduced. The usefulness of the techniques developed in this paper are demonstrated using experimental data.**

***Index Terms*— parameter estimation, power quality, automotive electrical systems.**

I. BACKGROUND

Modern automobiles incorporate more actuators, heaters, and other electrical loads than have automobiles in the past. This proliferation of high current, high power loads is presently challenging the longstanding assumption that the entire chassis will remain at one potential under a variety of different operating conditions. New voltage standards, alternator designs, and power electronics ensure that sufficient electrical power will be available for next-generation automotive loads [1], [2]. This paper considers the less obvious problem of transient voltage distortion resulting from load currents in the automobile chassis. The model and methods developed in this paper could help designers avoid problems related to high-power loads and may be useful for locating intermittent shorts and other faults.

The structure of the chassis plays a pivotal role in the automobile electrical system. Most loads in the automobile are connected as illustrated in Fig. 1. Current is carried by wires from the positive terminal of the battery to the loads and returned through the chassis. Electrical connections to the chassis are made at locations called "bonding points."

This paper provides a multi-input, multi-output model of the electrical behavior of the chassis that can predict voltage distortion given currents flowing into the electrical bonding points. We can predict voltage distortion with a minimal number of sensors by combining this technique and the current disaggregation techniques developed in [3], [4]. This paper begins with a model characterizing the electrical behavior of a sheet of steel. The model is extended to predict the electrical behavior at the bonding points on an automotive chassis. A parameter identification method [5] for the model is given in Section II. Experimental results in Section III show the application of this model to voltage distortion prediction in a "body-in-white" Ford Sable automobile chassis.

II. MODEL SELECTION

The electrical behavior of a steel sheet is first characterized by using the test apparatus in Fig. 2. The damped ringing current waveform which results from a steplike voltage input, as shown in Fig. 3, suggests that the steel sheet behaves like an inductor and a resistor in series. Figure 3 also illustrates the relatively good agreement between the measured current and the current predicted by a resistor-inductor model. This resistor-inductor model corresponds well with physical intuition. The steel is expected to have some resistance, and an inductive component is also expected because current is flowing either in or near the ferromagnetic chassis [6]. This direct contribution to the inductance is supplemented by a contribution due to the loops created by the proximity of the current-carrying wires.

A discrete-time formulation of the model was used because the parameters of the model were estimated with sampled data. The discrete-time constitutive relationship between the voltage across the steel sheet and the current flowing through it is

$$\hat{v}[k] = \mathtt{a}i[k] + \mathtt{b}i[k-1] \tag{1}$$

where $\mathtt{a}$ and $\mathtt{b}$ are parameters. The predicted voltage $\hat{v}$ is generated by this discrete-time model, while v denotes the experimentally measured voltage. The model used to produce $\hat{v}$ can be thought of as a discretization of the continuous-time equation of the resistor-inductor model,

$$\hat{v}(t) = L\frac{di(t)}{dt} + Ri(t). \tag{2}$$

Figure 4 illustrates an electrical chassis model of the chassis based on the results of the single sheet. The four corners of the model correspond to the four bonding point on the chassis. Most loads in the automobile, such as brake lights and headlights, are connected to one of these four bonding points. The parameters $\mathtt{a}_i$ and $\mathtt{b}_i$ of the steel sheet models between each of the bonding points will differ, due to variations in the amount and shape of steel between each pair of bonding points.

C.R. Laughman and S.B. Leeb are with the Laboratory for Electromagnetic and Electronic Systems, Massachusetts Institute of Technology, Cambridge, MA, 02139, USA.
S. R. Shaw is with Montana State University, Bozeman, MT 59717 USA.

0-7803-7906-3/03/$17.00 ©2003 IEEE.

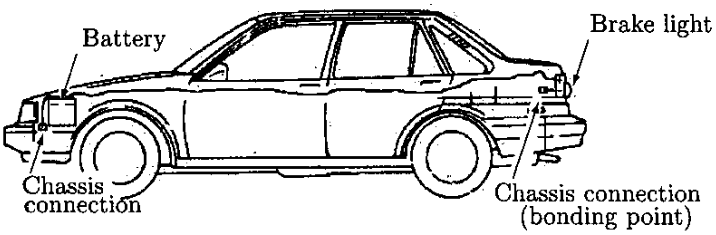

Fig. 1. Physical configuration of a representative electrical load.

III. Parameter Identification

The parameters of the the chassis model in Fig. 4 are identified by minimizing the loss function

$$g(\mu) = \sum_{k=1}^{N} (\mathbf{v}[k] - \hat{\mathbf{v}}_\mu[k])^2 \tag{3}$$

where $\mathbf{v}[k]$ represents the set of 6 measured voltages

$$\mathbf{v}[k] = \begin{bmatrix} v_{21}[k] \\ v_{23}[k] \\ v_{34}[k] \\ v_{14}[k] \\ v_{24}[k] \\ v_{13}[k] \end{bmatrix} \tag{4}$$

and $\hat{\mathbf{v}}_\mu[k]$ represents the set of 6 predicted voltages which depend on μ, the 6 pairs of parameters a_i and b_i of the chassis model. The constitutive equations for $\hat{\mathbf{v}}_\mu[k]$ can be written as

$$\begin{aligned} \hat{v}_{21}[k] &= \mathsf{a}_1 i_1[k] + \mathsf{b}_1 i_1[k-1] & (5)\\ \hat{v}_{23}[k] &= \mathsf{a}_2 i_2[k] + \mathsf{b}_2 i_2[k-1] & (6)\\ &\vdots \\ \hat{v}_{13}[k] &= \mathsf{a}_6 i_6[k] + \mathsf{b}_6 i_6[k-1] & (7) \end{aligned}$$

A method for simulating the voltage distortion by using a current measurement and an initial set of chassis model parameters is thus needed to construct $g(\mu)$. The core of this simulation method lies in solving a complete set of node and loop equations, examples of which are given by Equations 8 and 9, for all of the branch currents and voltages corresponding to the chassis model in Fig. 4.

$$\begin{aligned} i_1 + i_2 + i_5 &= i_m & (8)\\ v_{21} + v_{14} - v_{24} &= 0 & (9) \end{aligned}$$

The matrix form of the full set of node equations is shown in Equation 10:

$$\begin{bmatrix} -1 & 0 & 0 & 1 & 0 & 1 \\ 1 & 1 & 0 & 0 & 1 & 0 \\ 0 & -1 & 1 & 0 & 0 & 1 \end{bmatrix} \begin{bmatrix} i_1 \\ i_2 \\ i_3 \\ i_4 \\ i_5 \\ i_6 \end{bmatrix}_{[k]} = \begin{bmatrix} 0 \\ i_m \\ 0 \end{bmatrix}_{[k]} \tag{10}$$

or, in more compact notation:

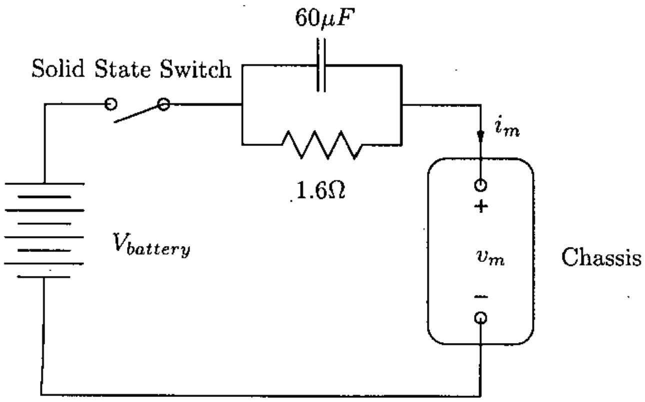

Fig. 2. Characterization current source.

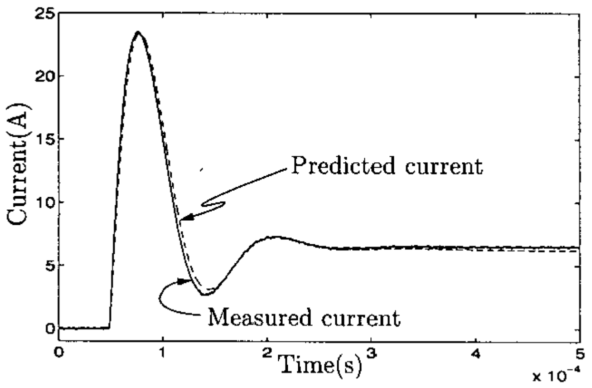

Fig. 3. Plot of the measured and predicted currents flowing through the steel sheet.

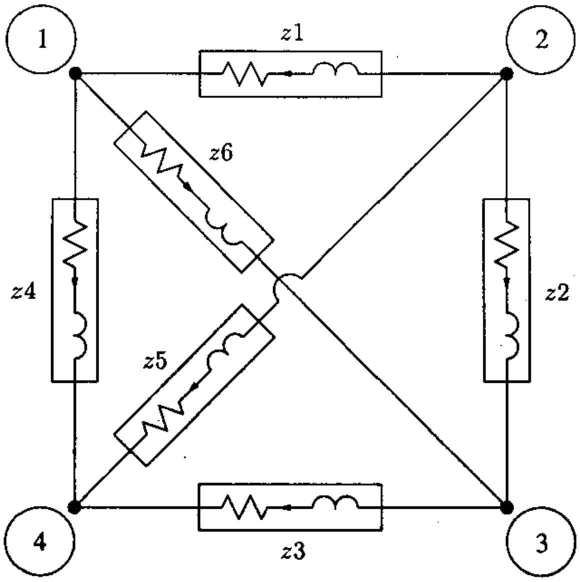

Fig. 4. A refined electrical model of the automobile chassis, representing its nature as an interconnection of steel panels.

$$\mathbf{A}\mathbf{i}[k] \;=\; \mathsf{b}[k]. \tag{11}$$

In comparison, the matrix form of the loop equations is given by Equation 12.

$$\mathbf{P}_{\mathsf{a}}\mathbf{i}[k] + \mathbf{P}_{\mathsf{b}}\mathbf{i}[k-1] = \mathbf{0} \tag{12}$$

where

$$\mathbf{P}_{\mathsf{a}} = \begin{bmatrix} \mathsf{a}_1 & 0 & 0 & \mathsf{a}_4 & -\mathsf{a}_5 & 0 \\ 0 & 0 & \mathsf{a}_3 & -\mathsf{a}_4 & 0 & \mathsf{a}_6 \\ -\mathsf{a}_1 & \mathsf{a}_2 & 0 & 0 & 0 & -\mathsf{a}_6 \end{bmatrix} \tag{13}$$

$$\mathbf{P}_{\mathsf{b}} = \begin{bmatrix} \mathsf{b}_1 & 0 & 0 & \mathsf{b}_4 & -\mathsf{b}_5 & 0 \\ 0 & 0 & \mathsf{b}_3 & -\mathsf{b}_4 & 0 & \mathsf{b}_6 \\ -\mathsf{b}_1 & \mathsf{b}_2 & 0 & 0 & 0 & -\mathsf{b}_6 \end{bmatrix}. \tag{14}$$

All of the above current and voltage constraints can be combined into Equation 15, which relates $\mathbf{i}[k]$ and $\mathbf{i}[k-1]$ to the source $\mathsf{b}[k]$.

$$\begin{bmatrix} \mathbf{A} \\ \mathbf{P}_{\mathsf{a}} \end{bmatrix} \mathbf{i}[k] + \begin{bmatrix} 0_{\mathrm{M}} \\ \mathbf{P}_{\mathsf{b}} \end{bmatrix} \mathsf{i}[k-1] = \begin{bmatrix} \mathsf{b}[k] \\ 0_{\mathsf{v}} \end{bmatrix} \tag{15}$$

A complete set of branch currents $\mathbf{i}[k]$ is needed to predict the voltages; by moving terms around as in Equation 16, these branch currents may be obtained by solving a conventional least squares problem. The QR decomposition is used to solve Equation 16, avoiding the poorly conditioned approach of solving the normal equations.

$$\begin{bmatrix} \mathbf{A} \\ \mathbf{P}_{\mathsf{a}} \end{bmatrix} \mathsf{i}[k] = \begin{bmatrix} \mathsf{b}[k] \\ 0_{\mathsf{v}} \end{bmatrix} - \begin{bmatrix} \mathbf{0}_{\mathrm{M}} \\ \mathbf{P}_{\mathsf{b}} \end{bmatrix} \mathsf{i}[k-1] \tag{16}$$

The process of computing $\mathbf{i}[k]$ begins by ensuring that the system is at rest (no current flowing) at the start of each dataset, so that $\mathbf{i}[0] = 0$. Solving for $\mathbf{i}[k]$ over $k = 1 : N$ then requires only the iteration of Equation 16 by using the measured current. Finally, the set of simulated voltage waveforms $\mathbf{v}$ can be created by applying the pertinent constitutive equations:

$$\begin{bmatrix} \hat{v}_{21} \\ \hat{v}_{23} \\ \hat{v}_{34} \\ \hat{v}_{14} \end{bmatrix}_{[k]} = \alpha \begin{bmatrix} i_1 \\ i_2 \\ i_3 \\ i_4 \end{bmatrix}_{[k]} + \beta \begin{bmatrix} i_1 \\ i_2 \\ i_3 \\ i_4 \end{bmatrix}_{[k-1]}. \tag{17}$$

$$\alpha \;=\; \mathrm{diag}(\mathsf{a}_1, \mathsf{a}_2, \mathsf{a}_3, \mathsf{a}_4) \tag{18}$$

$$\beta \;=\; \mathrm{diag}(\mathsf{b}_1, \mathsf{b}_2, \mathsf{b}_3, \mathsf{b}_4). \tag{19}$$

The parameters of the chassis may now be identified by comparing the simulated voltage distortion with the measured voltage distortion. While we assumed that the initial guess of the parameters μ_0 produced the correct voltage predictions, this will not usually be the case. This μ_0 is refined by using the first simulation of the voltage distortion $\hat{\mathbf{v}}_\mu$ and the measured voltage distortion $\mathbf{v}$ to construct $g(\mu)$. The Levenberg-Marquardt nonlinear least squares algorithm [7] is used to repeatedly refine μ and recalculate $\hat{\mathbf{v}}_\mu$ until the simulated voltage distortion is acceptably close to the set of measured voltages $\mathbf{v}$.

Although the best parameter estimates will be produced when all of the possible voltage measurements are made, a subset of voltage waveforms can also be used to generate a set of parameters. For example, if only v_{21}, v_{23}, and v_{34} are measured, a set of parameters for all 6 branches may still be obtained with the same parameter estimation method with only a small modification to the residual's structure. These parameters estimates do not characterize the electrical behavior of the chassis as well as those parameters obtained using the voltages measured along all four branches.

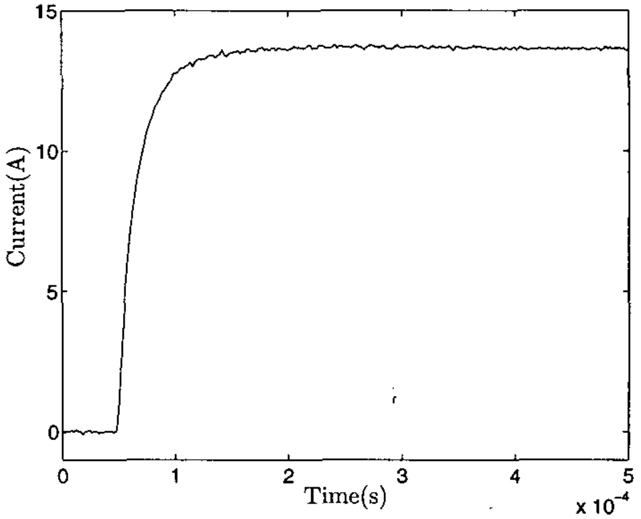

Fig. 5. Current transient injected into node 2 with an excitation from the headlight.

The sampling period T_s used during the acquisition of the current and voltage data also affects the estimated parameters. In particular, if T_s is chosen to be too small, the parameter estimates will be extremely sensitive to noise. The value of T_s which we used was $2\mu s$.

IV. RESULTS

Voltages v_{14}, v_{21}, v_{23}, and v_{34} (as seen in Fig. 4) were measured with ADA400 differential preamplifiers, while the current injected into node 2 was measured with a Tektronix A6303 current probe and AM503B current probe amplifier. The current was returned from node 4, which corresponded to the front right corner of the car. All of the waveforms were acquired with a Tektronix TDS744A oscilloscope.

Two different sets of data were obtained. The first was used for the purposes of generating a set of parameter estimates, while the second was used to validate these estimates. The first dataset was excited via the setup illustrated in Fig. 2. The size of the capacitor was adjusted to produce sufficient dynamics to support good estimates of both the inductive and the resistive effects.

The validation dataset excited the transients by using a setup similar to that in Fig. 2, with a Wagner halogen headlamp replacing the capacitor and resistor. A headlamp was used to validate the test apparatus because the ability to predict the voltage distortion caused by a headlight is immediately applicable to the modern automobile. A representative headlight current transient can be seen in Fig. 5, and the accompanying voltage transients and predictions can be seen respectively in Figs. 6, 7, 8, and 9. The noise observed on these voltage predictions is an artifact of the numerical method used to obtain the branch currents for the predictions. The predicted voltages

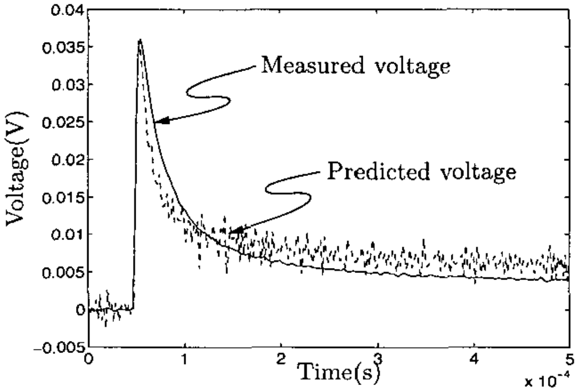

Fig. 6. Plot of v_{21} resulting from a current excitation from the headlight injected into node 2.

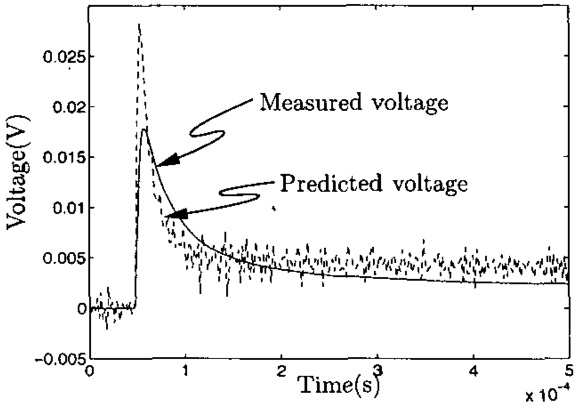

Fig. 7. Plot of v_{23} resulting from a current excitation from the headlight injected into node 2.

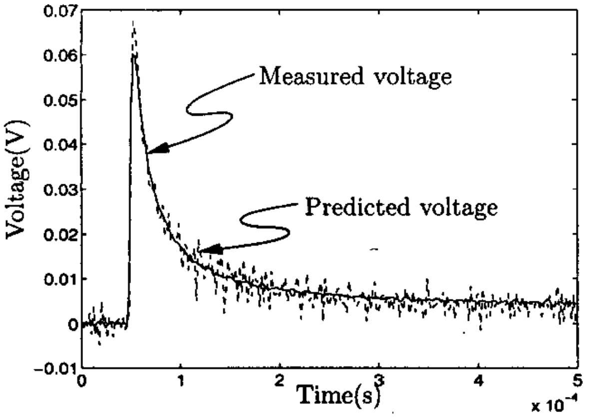

Fig. 8. Plot of v_{34} resulting from a current excitation from the headlight injected into node 2.

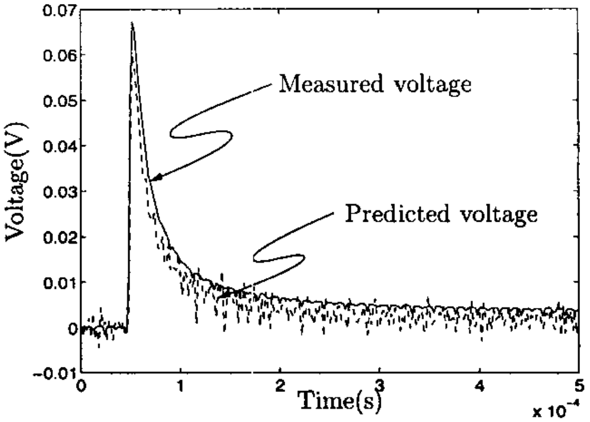

Fig. 9. Plot of v_{14} resulting from a current excitation from the headlight injected into node 2.

closely match the observed voltage distortion, indicating that the model may successfully be used to predict voltage distortion at many points in the body, by only measuring the current flowing at one point.

V. DISCUSSION

We have demonstrated the success of applying the discussed modeling techniques to the automobile chassis for the purposes of the prediction of voltage distortion. This model is particularly relevant because it can predict the voltage distortion created at many bonding points when a current is injected into only one bonding point. We anticipate that this model of the automobile electrical system will be useful in many applications, such as the precise location of intermittent wiring faults.

ACKNOWLEDGEMENTS

This research was funded by The Grainger Foundation, The U.S. Navy, the Ford Motor Company, a CAREER award from the National Science Foundation, and MIT's Carl Richard Soderberg Career Development Chair.

REFERENCES

[1] J.G. Kassakian, D.J. Perreault, "The Future of Electronics in Automobiles," *Proceedings of the 13th International Symposium on Power Semiconductor Devices and ICs*, June 4-7, 2001.

[2] J.G. Kassakian, J.M. Miller, N. Traub, "Automotive Electronics Power Up," *IEEE Spectrum*, May 2000.

[3] S.R. Shaw, *"System Identification Techniques and Modeling for Nonintrusive Load Diagnostics,"* Ph.D., MIT, Department of Electrical Engineering and Computer Science, February 2000.

[4] S.R. Shaw, D.J. Evangelista, S.B. Leeb, C.R. Laughman, "Non-Intrusive Load Monitoring and Identification in an Automotive Environment," *6th Annual ElectrIMACS Conference*, Sept 14-16, 1999, Lisbon, Portugal.

[5] C.R. Laughman, *"Parameter Identification and Modelling for the Prediction of Voltage Distortion,"* M.Eng, MIT, Department of Electrical Engineering and Computer Science, June 2001.

[6] R.M. Bozorth, *Ferromagnetism.* Van Nostrand Company, Inc., 1951.

[7] G.A.F Seber and C.J. Wild. *Nonlinear Regression.* Probability and Mathematical Statistics. Wiley, 1989.